Hydrolysis of ATP by Polymerized Actin Depends on the Bound Divalent Cation but Not Profilin†

Laurent Blanchoin‡ and Thomas D. Pollard*

Structural Biology Laboratory, The Salk Institute for Biological Studies, 10010 North Torrey Pines Road, La Jolla, California 92037

Received June 12, 2001; Revised Manuscript Received October 2, 2001

ABSTRACT: Growing evidence suggests that the nucleotide bound to actin filaments serves as a timer to control actin filament turnover during cell motility (Pollard, T. D., Blanchoin, L., and Mullins, R. D. (2000) *Annu. Rev. Biophys. Biomol. Struct. 29*, 545−576). We re-examined the hydrolysis of ATP by polymerized actin using mechanical quenched-flow methods to improve temporal resolution. The rate constant for ATP hydrolysis by polymerized Mg actin is 0.3 s^{-1}, 3-fold faster than that measured manually. The ATP hydrolysis rate is similar when Mg ATP actin elongates either the pointed end or the barbed end of filaments. Polymerized Ca actin hydrolyzes ATP at 0.05 s^{-1}. Mg ATP actin saturated with profilin can elongate barbed ends at >60 s^{-1}, 2 orders of magnitude faster than ATP hydrolysis (0.3 s^{-1}). Given that profilin binds to a surface on actin that is buried in the Holmes model of the actin filament, we expect that profilin will block subunit addition at the barbed end of a filament. Profilin must move from this site at rates much faster than it dissociates from monomers (4 s^{-1}). ATP hydrolysis is not required for this movement.

Although bound nucleotide is not required for actin polymerization (*2*, *3*), hydrolysis of ATP and dissociation of the γ-phosphate appear to trigger actin filament turnover by regulatory proteins during cell motility. Our current understanding is that the Arp2/3 complex initiates filament branches that grow in the barbed direction by the addition of Mg ATP actin (*4*−*5*). Subsequent hydrolysis of ATP and phosphate dissociation promote dissociation of branches (*6*) and allow ADF/cofilins to sever ADP filaments and to promote their disassembly (*6*−*7*).

The first step in this chain of events is the hydrolysis of ATP bound to polymerized actin. For years after the reaction was discovered (*8*), ATP hydrolysis was thought to be coupled to incorporation of ATP actin at the ends of growing filaments. Eventually, a lag was observed between subunit incorporation and hydrolysis (*9*), but in subsequent work (*10*, *11*), resolution of the two events during the time course of polymerization proved to be right at the limit of manual methods to record the time course of hydrolysis (Table 1). ATP hydrolysis is irreversible by rigorous criteria (*12*).

Interpretation of kinetic data on nucleotide hydrolysis depends on the model assumed for the hydrolysis process. The simplest assumption is that each polymerized ATP actin molecule hydrolyzes its ATP independently in a first-order reaction that is not strongly influenced by the nucleotide bound to surrounding subunits (*10*). Alternatively, neighboring subunits might influence hydrolysis. One model is that hydrolysis is strongly favored at the boundary between a central core of ADP subunits or ADP−P_i subunits and caps of newly added ATP subunits, a vectorial hydrolysis model proposed for Mg ATP actin but not for Ca ATP actin (*11*). Because only one subunit per end is in this special environment, the rate of hydrolysis on this subunit would have to be very much faster than that on random subunits acting independently. The random and vectorial hydrolysis mechanisms are difficult to distinguish with kinetic data, so Pieper and Wegner (*13*) tested them by copolymerizing mixtures of ATP actin and ADP actin. They assumed that the presence of ADP subunits would increase the rate of hydrolysis by neighboring ATP subunits if the vectorial hydrolysis mechanism were correct. They found that the presence of ADP subunits had no influence on the rate of hydrolysis, consistent with but not proving the random hydrolysis mechanism. One question about their experiment is the unusually low rate of hydrolysis (*13*). Nevertheless, in the absence of better data, we assume that hydrolysis is random and influenced little or not at all by the nucleotide state of adjacent subunits. This assumption is also consistent with the fact that phosphate dissociation is slow (*14*) and ADP−P_i and ATP actin are indistinguishable (*15*). Thus, at the time of hydrolysis, ATP

Table 1. Rate Constants for ATP Hydrolysis by Polymerized Actin[a]

Mg ATP actin	Ca ATP actin	Li ATP actin	ref
	0.0005		*9*
0.07[b]	0.08		*10*
0.08	0.02		*16*
0.02	0.01		*13*
0.30	0.05	0.30	current work

[a] Units are s^{-1}. [b] Ca ATP actin polymerized in $MgCl_2$ and EGTA, resulting in a mixture of Mg and Ca ATP actin.

† This work was supported by NIH research Grant GM-26338 to T.D.P.

* Corresponding author: Tel: 203-432-3565: Fax: 203-432-6161. Email: thomas.pollard@yale.edu. Current address: Department of Molecular, Cellular and Developmental Biology, Yale University, New Haven, CT 06520-8103.

‡ Current address: Laboratoire de Physiologie Cellulaire Végétale, CEA Grenoble, 38054 Grenoble cedex 9, France.

10.1021/bi011214b CCC: $22.00
Published on Web 12/14/2001

subunits will usually be flanked by ATP or ADP−P_i subunits rather than by ADP subunits.

We re-examined the hydrolysis of ATP by polymerized actin using mechanical quenched-flow methods to improve reproducibility and temporal resolution. We find that hydrolysis by Mg ATP actin is 3 times faster than that measured with manual methods. For the first time, we show that hydrolysis at the pointed end is similar to that at the barbed end. Further, saturating concentrations of profilin do not affect the hydrolysis rate of subunits incorporated at the barbed end. Elongation can exceed hydrolysis by more than 2 orders of magnitude, showing that elongation by profilin−actin and hydrolysis are not coupled.

EXPERIMENTAL PROCEDURES

Reagents. Materials came from the following sources: dithiothreitol (DTT), EDTA, Tris, sodium azide, ATP, ADP, and phalloidin from Sigma Chemical Company (St. Louis, MO); silicotungstic acid and isobutanol from Aldrich Chemical Co. (St. Louis, MO); ^{32}P-γ-ATP from NEN (Boston, MA); ammonium molybdate from J. T. Baker (Philipsburg, NJ).

Proteins. Actin was isolated from rabbit skeletal muscle acetone powder (*17*) or from *Acanthamoeba* (*18*). Monomeric Ca ATP actin was purified by gel filtration on Sephacryl S-300 (*19*) at 4 °C in the G buffer (5 mM Tris-Cl (pH 8.0), 0.2 mM ATP, 0.1 mM $CaCl_2$, and 0.5 mM DTT). Actin was labeled on Cys374 to a stoichiometry of 0.8−1.0 with pyrene iodoacetamide (*20*; modified by ref *18*). Mg ATP actin was prepared on ice by treating Ca ATP actin with a Dowex resin (AG 1-X4 resin; Bio-Rad, Randolph, MA) to remove free ATP from the G buffer and then adding 0.2 mM EGTA and an 11-fold molar excess of $MgCl_2$ over actin for 5 min, and the solution was used within hours. Actin was polymerized by the addition of 1:9 (v/v) of 10X KME (500 mM KCl, 10 mM $MgCl_2$, 10 mM EGTA, and 100 mM Tris-Cl (pH 7.0)). Mg ^{32}P-γ-ATP actin was prepared by incubating dowexed Ca ATP actin with a 10-fold excess of ^{32}P-γ-ATP and an 11-fold molar excess of $MgCl_2$ in 0.2 mM EGTA for 30 min on ice. Free ^{32}P-γ-ATP was removed by two treatments with the Dowex resin. *Acanthamoeba castellanii* profilin-I was purified according to Kaiser et al. (*21*). Human profilin was expressed in *Escherichia coli* and purified (*22*). Both profilins inhibited elongation from the pointed end of gelsolin actin seeds (*4*). Spectrin actin seeds were purified from human red blood cells (*23*).

Elongation Assay. Equal volumes of 6 μM unlabeled actin filaments in the 2X F0 buffer (100 mM KCl, 2 mM $MgCl_2$, 2 mM EGTA, 0.5 mM DTT, and 15 mM Tris-Cl (pH 7.0)) and 6 μM actin monomers in the G0 buffer (5 mM Tris-Cl (pH 7.0), 0.5 mM DTT, and 1 mM azide) partially labeled with pyrene (5%) were mixed rapidly (Mini Stopped-Flow; Kintek Corporation, Austin, TX) at 25 °C, and the time course of polymerization was recorded by the change in pyrene fluorescence. The rate of polymerization is proportional to the number concentration of actin filaments [N] according to

$$\text{rate} = k_+[\text{A}][\text{N}] - k_-[\text{N}] \quad (1)$$

where k_+ is the association rate constant, k_- is the dissociation rate constant, and [A] is the concentration of actin monomers.

ATP Hydrolysis. Equal volumes of 6 μM polymerized actin in the 2X F0 buffer and 6 μM actin monomers labeled with ^{32}P-γ-ATP in the G0 buffer were mixed rapidly and quenched at a series of time points with an equal volume of silicotungstic−sulfuric acid (4.3% aqueous silicotungstic acid and 2.8 N sulfuric acid) using a Chemical Quench-Flow (model RQF-3; Kintek Corporation, Austin, TX). Samples were recovered in glass tubes containing 1 mL of 1:1 isobutanol/xylene and immediately vortexed with 0.1 mL of 10% ammonium molybdate for 20 s. The yellow phospho−molybdate complex was extracted quantitatively into the organic phase (*24, 25*), and an aliquot was counted. ATP or ADP remain in the lower aqueous phase.

Data Analysis and Simulation of Kinetics. We used KINSIM (*26*) to simulate the time course of actin filament elongation and ATP hydrolysis.

RESULTS

Experimental Design. To improve the temporal resolution relative to previous studies (*10, 11, 16, 27*), we used a quenched-flow apparatus to follow the time course of ATP hydrolysis by polymerized actin. Actin monomers with bound ^{32}P-γ-ATP were polymerized by elongation of actin filament seeds, either uncapped to observe the events at the barbed end or with barbed ends capped with gelsolin to observe the events at the pointed end. The time course of polymerization was documented by the change of fluorescence of a trace of pyrenyl actin using a stopped-flow apparatus with the same mixer as the quenched-flow apparatus. Identical samples were mixed and quenched at various time points with acid to stop ATP hydrolysis and to release inorganic phosphate from actin.

We determined ATP hydrolysis rate constants by simulating the time courses of polymerization and ATP hydrolysis using the reactions in model 1:

$$\text{A} + \text{N} \leftrightarrow \text{AT} + \text{N}$$

$$\text{AT} \leftrightarrow \text{AD} + \text{P}$$

where A is the actin monomer, N is the concentration of filament ends, AT is polymerized ATP actin, AD is polymerized ADP actin, and P is inorganic phosphate, either bound to actin or dissociated. The rate of polymerization (reaction 1) is equal to the product of the association rate constant (k_+), the concentration of monomers, and the concentration of filament ends. For uncapped filaments, we used barbed end association rate constants $k_+ = 10\ \mu\text{M}^{-1}\ \text{s}^{-1}$ for Mg ATP actin and $4.8\ \mu\text{M}^{-1}\ \text{s}^{-1}$ for Ca ATP actin (*28*). For gelsolin-capped filaments, we used the pointed end association rate constant for Ca ATP actin, $k_+ = 1.3\ \mu\text{M}^{-1}\ \text{s}^{-1}$. We set the dissociation rate constants to zero, because dissociation is much slower than elongation under our conditions. ATP hydrolysis by actin is irreversible (*12*), so we set the rate constant for ATP synthesis to zero. We searched for the concentration of filament ends and the ATP hydrolysis rate constant giving simulations that best fit the two time courses.

Effect of Cations on ATP Hydrolysis by Polymerized Actin. Elongation of Mg ATP actin from preformed actin filament seeds followed an exponential time course (Figure 1A), so the concentration of filament ends was nearly constant during

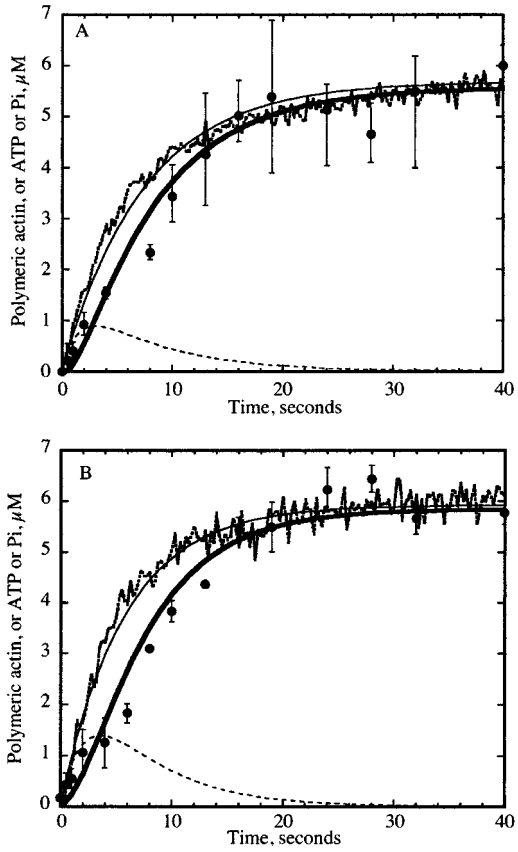

FIGURE 1: ATP hydrolysis by Mg ATP actin and Li ATP actin grown from the barbed ends of actin filaments. (A) Polymerization of 6 μM Mg ATP actin monomers from 6 μM Mg ADP actin filament seeds. Conditions: 10 mM Tris-Cl (pH 7.0), 50 mM KCl, 1 mM $MgCl_2$, 0.2 mM ATP, 0.5 mM DTT, and 3 mM NaN_3 at 25 °C. The dotted noisy line is the time course of polymerization. Simulation of this reaction (smooth curve, total polymer) gave a concentration of 11.2 nM filament ends, corresponding to an average initial length of 1.6 μm or 535 subunits. Circles are the time course of ATP hydrolysis followed by $^{32}P_i$ released from ^{32}P-γ-ATP bound to the actin monomers for muscle actin (closed circles). The dashed line is simulation of the concentration of ATP polymer, and the solid thick line is simulation of ATP hydrolysis using a hydrolysis rate constant of 0.3 s^{-1}. (B) Polymerization of 6 μM Li ATP actin monomers from 6 μM Li ADP actin filament seeds. Conditions: 2 mM MOPS (pH 7.0), 50 mM KCl, 400 μM LiCl, 0.2 mM ATP, 0.5 mM DTT, and 1 mM NaN_3. The dotted noisy line is the time course of polymerization. Simulation of this reaction (smooth curve, total polymer) gave a concentration of 13.6 nM filament ends, corresponding to an average initial length of 1.3 μm or 441 subunits. Closed circles are the time course of ATP hydrolysis. The dashed line is simulation of the concentration of ATP polymer, and the solid thick line is simulation of ATP hydrolysis using a hydrolysis rate constant of 0.3 s^{-1}.

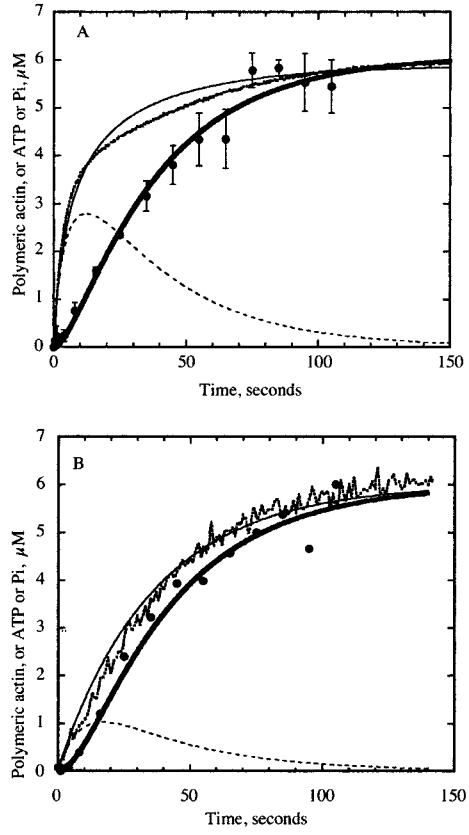

FIGURE 2: ATP hydrolysis by Ca ATP actin grown from the barbed ends of actin filaments or spectrin actin seeds. Conditions: 10 mM Tris-Cl (pH 7.0), 50 mM KCl, 1 mM $CaCl_2$, 0.2 mM ATP, 0.5 mM DTT, and 3 mM NaN_3 at 25 °C. (A) Polymerization of 6 μM Ca ATP actin monomers from 6 μM Ca ADP actin filament seeds. The dotted noisy line is the time course of polymerization. Simulation of this reaction (smooth curve, total polymer) gave an initial concentration of 18 nM filament ends, corresponding to an initial average length of 1.1 μm or 333 subunits. Closed circles are the time course of ATP hydrolysis. The dashed line is simulation of the concentration of ATP polymer, and the solid thick line is simulation of ATP hydrolysis using a hydrolysis rate constant of 0.05 s^{-1}. (B) Polymerization of 6 μM Ca ATP actin monomers from 2.3 nM spectrin actin seeds. The dotted noisy line is the time course of polymerization. Closed circles are the time course of ATP hydrolysis. The dashed line is simulation of the concentration of ATP polymer, and the solid thick line is inorganic phosphate using a hydrolysis rate constant of 0.05 s^{-1}.

the experiment. ATP hydrolysis followed closely behind polymerization with a rate constant of 0.3 ± 0.1 s^{-1}, much faster than the original report (*9*) and 3-fold faster than subsequent reports with a manual collection of time points (*10*, *11*). Results with Li ATP actin were indistinguishable (Figure 1B). A rapid mixer was essential to detect the small lag between elongation and ATP hydrolysis for both Li actin and Mg actin.

Although seeded polymerization of Ca ATP actin monomers followed an exponential time course when the reactants were hand mixed, the time course deviated from an exponential curve following rapid mixing. Elongation slowed progressively relative to an exponential, indicating that the concentration of filament ends declined with time (Figure 2A). Extensive microscopic and kinetics experiments established that annealing accounts for the deviation of the Ca ATP actin curves from a simple exponential (*29*). Accordingly, the time course of elongation of Ca ATP actin from spectrin actin seeds deviated less from an exponential (Figure 2B), because these seeds are blocked on their pointed ends, precluding annealing. It was not practical to use spectrin actin seeds for routine ATP hydrolysis experiments, because high concentrations of seeds were required to achieve polymerization fast enough to resolve the lag between polymerization and ATP hydrolysis.

The addition of an annealing step ($N + N \leftrightarrow N$) to model 1 improved the fit of the model to the Ca ATP actin polymerization time course and yielded a rate constant for ATP hydrolysis by polymerized Ca ATP actin of 0.05 ± 0.02 s^{-1}, in good agreement with previous reports (*10*, *11*). Polymerization of Ca ATP actin in the KMEI buffer

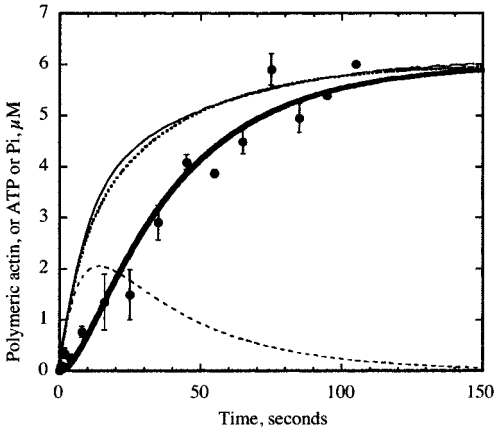

FIGURE 3: ATP hydrolysis by Ca ATP actin polymerized at the pointed ends of actin filaments. Conditions: 10 mM Tris-Cl (pH 7.0), 50 mM KCl, 1 mM $CaCl_2$, 0.2 mM ATP, 0.5 mM DTT, and 3 mM NaN_3 at 25 °C. The noisy line is the time course of polymerization of 6 μM Ca ATP actin monomers from 22.4 nM gelsolin actin seeds. The dotted line is the time course of polymerization. Closed circles are the time course of ATP hydrolysis. The dashed line is simulation of the concentration of ATP polymer, and the solid thick line is simulation of ATP hydrolysis using a hydrolysis rate constant of 0.05 s^{-1}.

containing $MgCl_2$ and EGTA resulted in a rate of ATP hydrolysis of 0.15 ± 0.05 s^{-1}, between the rate of ATP hydrolysis for pure Mg actin and pure Ca actin. This is a consequence of the slow exchange of Ca^{2+} for Mg^{2+} during polymerization.

ATP Hydrolysis at the Pointed Ends of Actin Filaments. ATP hydrolysis occurs after the addition of ATP actin to the pointed end of actin filaments (*30*), but the rate of the reaction had not been measured. It was important to determine if hydrolysis is coupled directly to subunit addition or occurs after polymerization as at the barbed end. ATP hydrolysis at the pointed end is important, because the bound nucleotide controls dissociation of pointed ends from the Arp2/3 complex (*6*).

We measured the time course of ATP hydrolysis by actin subunits added to the pointed ends of gelsolin-capped actin filaments (Figure 3). The time course of elongation was exponential, because short capped seeds were not fragmented by the mixer and could not anneal. ATP hydrolysis lagged behind polymerization, and the simulation gave a hydrolysis rate constant of 0.05 ± 0.01 s^{-1} for polymerized Ca ATP actin, similar to that of the barbed end. We could not measure accurately the rate of hydrolysis of Mg ATP actin polymerized on the pointed ends. Rapid hydrolysis kept up with the slow pace of elongation, so we could not resolve the time courses of elongation and hydrolysis. The minimum value of the Mg ATP hydrolysis rate constant was 0.1 s^{-1}, similar to the rate constant at the barbed end.

ATP Hydrolysis at the Barbed Ends in the Presence of Profilin. Profilin−actin complexes elongate the barbed ends of actin filaments nearly as fast as actin monomers (*31, 32*). Only at free profilin concentrations far higher than those required to saturate all Mg ATP actin monomers does elongation slow to about 80% of the rate of actin alone (*32, 33*). Two hypotheses have been proposed to explain these observations. A barbed end capping hypothesis (*31, 33, 34*) suggests that profilin has a much lower affinity for barbed ends than for actin monomers, dissociating rapidly from barbed ends after the addition of the complex and only slowing elongation at free profilin concentrations that allow for occupancy of the barbed ends. Pantaloni and Carlier (*35*) questioned this model on thermodynamic grounds and proposed that profilin dissociation from barbed ends is coupled to ATP hydrolysis on the terminal subunit. However, a thermodynamic analysis of actin assembly in the presence of profilin and thymosin β_4 showed that ATP hydrolysis was not required for elongation by profilin−actin (*36*).

An independent way to distinguish these models would be to test if ATP hydrolysis limits the rate of barbed end elongation by profilin−actin complexes. This was impossible with manual methods but was feasible with quenched-flow mixing. We confirmed that a 4-fold excess of neither human nor amoeba profilin inhibits the elongation of Mg ATP muscle actin at barbed ends over a range of actin concentrations (Figure 4A). Without and with excess profilin, the elongation rate was directly proportional to the actin concentration. Elongation of 6 μM Mg ATP actin with 24 μM amoeba profilin (a concentration 200-fold higher than the K_d for actin) followed an exponential time course, with hydrolysis of bound ATP clearly lagging behind polymerization (Figure 4B). The hydrolysis rate constant was 0.3 s^{-1}, far slower than the initial elongation rate of 60 s^{-1}. Thus, profilin does not influence the hydrolysis rate, and many profilin−actins add to barbed ends before ATP hydrolysis on terminal subunits. The lag between subunit incorporation at the barbed end and ATP hydrolysis was larger for Ca ATP actin than for Mg ATP actin (Figure 4C). The ATP hydrolysis rate constant for Ca ATP actin with saturating profilin was 0.055 s^{-1}, the same as that without profilin.

DISCUSSION

After polymerization, Mg ATP actin hydrolyzes bound ATP with a rate constant of 0.3 s^{-1}, assuming that hydrolysis by polymerized subunits is random. This measurement is challenging, even with quenched-flow equipment, because the time course of elongation, the prerequisite to observing hydrolysis, is limited by the concentration of filament ends. Regardless of the concentration of monomers, the elongation reaction is a pseudo-first-order process with a rate constant equal to the product of the elongation rate constant and the concentration of ends. Even with the rapid mixer fragmenting 6 μM polymerized actin into 1 μm segments, the elongation rate constant was only 0.14 s^{-1}. Thus, irrespective of the concentration of monomers, the half-time for polymerization is 5 s, about the same as the 2 s half-time for hydrolysis. Higher concentrations of filaments increase the bulk rate of polymerization but are more difficult to mix.

The rate of ATP hydrolysis by polymerized actin depends on the divalent cation bound to the high-affinity site (Table 1). The physiologically relevant species, Mg ATP actin, hydrolyzes ATP 6 times faster than Ca ATP actin. Literature values are more consistent for Ca ATP actin than for Mg ATP actin. This is attributable to the great difficulty of measuring the fast Mg ATPase rates manually. In addition, Mg^{2+} was not fully exchanged for Ca^{2+} prior to assembly in our earlier work (*10*). Polymerization of Ca ATP actin in $MgCl_2$ and EGTA results in only a partial exchange of divalent cations during the elongation reaction and an intermediate rate of ATP hydrolysis.

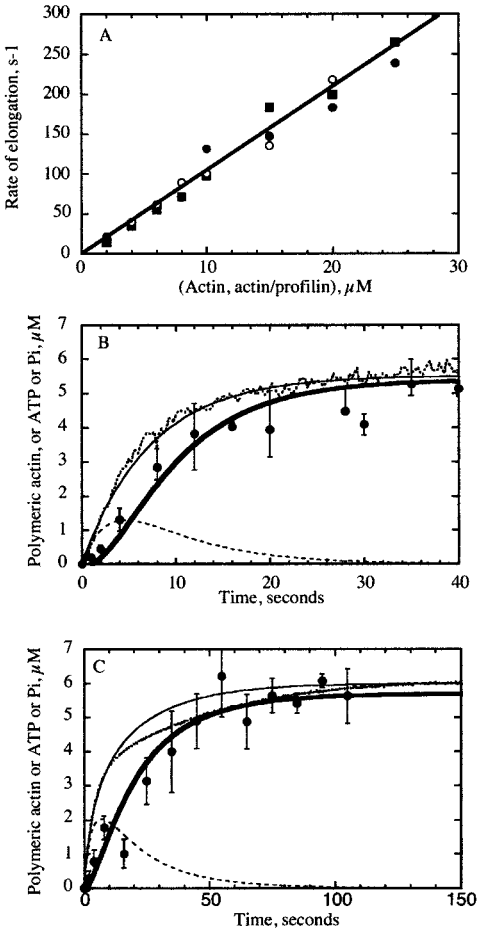

FIGURE 4: Elongation and ATP hydrolysis by profilin−actin complexes. (A) Dependence of the rate of elongation on the concentration of Mg ATP actin alone (closed squares), with a 4-fold molar excess of human profilin-I (closed circles), or with a 4-fold molar excess of amoeba profilin-I (open circles) relative to actin. Conditions: 10 mM Tris-Cl (pH 7.0), 50 mM KCl, 1 mM $MgCl_2$, 0.2 mM ATP, 0.5 mM DTT, 3 mM NaN_3 at 25 °C, and 6 μM Mg ADP actin filament seeds. (B) Polymerization of 6 μM Mg ATP actin monomers with 24 μM amoeba profilin-I from 6 μM Mg ADP actin filaments seeds. The dotted noisy line is the time course of polymerization. Simulation of this reaction (smooth curve, total polymer) gave a concentration of 11.6 nM filament ends corresponding to an average initial length of 1.55 μm or 517 subunits. Closed squares are the time course of ATP hydrolysis followed by $^{32}P_i$ released from ^{32}P-γ-ATP bound to the actin monomers. The dashed line is simulation of the concentration of ATP polymer, and the solid thick line is simulation of ATP hydrolysis using a hydrolysis rate constant of 0.3 s^{-1}. (C) Polymerization of 6 μM Ca ATP actin monomers with 24 μM amoeba profilin-I from 6 μM Ca ADP actin filaments seeds. The dotted noisy line is the time course of polymerization. Simulation of this reaction (smooth curve, total polymer) gave a concentration of 14.5 nM filament ends, corresponding to an average initial length of 1.2 μm or 405 subunits. Closed circles are the time course of ATP hydrolysis. The dashed line is simulation of the concentration of ATP polymer, and the solid thick line is simulation of ATP hydrolysis using a hydrolysis rate constant of 0.055 s^{-1}.

We measured ATP hydrolysis by Li ATP actin, because structural observations (Vorobiev, S., and Almo, S. C., personal communication) suggest a mechanism for ATP hydrolysis where attack by a water molecule depends on the bound divalent cation, with Li^{2+} being more favorable than Mg^{2+} and Ca^{2+} being the least favorable. Our time resolution sufficed to show that Li and Mg ATP actin hydrolyzed ATP faster than Ca ATP actin but not to detect a difference between Mg and Li ATP actin.

Saturating actin monomers with profilin neither limits the rate of elongation nor alters the rate of ATP hydrolysis by polymerized Mg ATP actin. Profilin binds actin monomers on a surface (*37*) that is buried in the Holmes model of the actin filament (*38*). When bound to this site, profilin is presumed to block the addition of subunits to the barbed end of an actin filament. Therefore, profilin must move out of the way before the next subunit binds. In principle, this movement could be either to a secondary binding site on the surface of the filament or complete dissociation. Profilin binding to ADP actin filaments was not detected by a sensitive fluorescence anisotropy assay (*39*), so the affinity of profilin for the sides of actin filaments is very low. Because profilin−actin can elongate barbed ends at a rate of more the 60 subunits per second, profilin must move out of the way at a rate much faster than it dissociates from actin monomers (4 s^{-1}; *39*, *40*). One hypothesis is that ATP hydrolysis causes a conformational change in actin, which favors the movement of profilin (*32*). However, the addition of profilin−actin to barbed ends can exceed the rate of hydrolysis by more than 2 orders of magnitude. Therefore, profilin movement occurs on ATP actin and may result from a conformational change driven by the free-energy change accompanying profilin−actin binding to the end of the filament. We think that profilin dissociates directly from the end of the filament. However, if profilin moves to a secondary site on the side of the filament, the subsequent hydrolysis of ATP and phosphate release might contribute to the dissociation of profilin from this secondary site and account for the undetectable affinity of profilin for the sides of ADP actin filaments.

ATP hydrolysis by polymerized Mg ATP actin is faster (0.3 s^{-1}) than the rate of actin filament turnover in vivo, so hydrolysis is not expected to be rate limiting in the cycle of actin assembly and disassembly. The product of irreversible ATP hydrolysis is a long-lived intermediate, ADP−P_i actin, which appears to have properties identical to those of ATP actin (*15*). The key event after ATP hydrolysis is phosphate dissociation that induces a conformational change in actin (*41*, *42*), because phosphate dissociation limits the binding of ADF/cofilin to ADP actin filaments and controls dissociation branches from the Arp2/3 complex (*6*). Phosphate dissociation may be rate limiting in cells, but ADF/cofilin accelerates this reaction (*43*).

ACKNOWLEDGMENT

The authors thank Don Kaiser for *Acanthamoeba* profilin and Dr. Enrique De La Cruz for suggestions during the course of this investigation.

REFERENCES

1. Pollard, T. D., Blanchoin, L., and Mullins, R. D. (2000) *Annu. Rev. Biophys. Biomol. Struct. 29*, 545−576.
2. Kasai, M. (1969) *Biochim. Biophys. Acta 180*, 399−409.
3. De La Cruz, E. M., Mandinova, A., Steinmetz, M. O., Stoffler, D., Aebi, U., and Pollard, T. D. (2000) *J. Mol. Biol. 295*, 517−526.
4. Mullins, R. D., Heuser, J. A., and Pollard, T. D. (1998) *Proc. Natl. Acad. Sci. U.S.A. 95*, 6181−6186.
5. Pantaloni, D., Boujemaa, R., Didry, D., Gounon, P., and Carlier, M.-F. (2000) *Nat. Cell Biol. 2*, 385−391.
6. Blanchoin, L., Pollard, T. D., and Mullins, R. D. (2000) *Curr. Biol. 10*, 1273−1282.

7. Didry, D., Carlier, M. F., and Pantaloni, D. (1998) *J. Biol. Chem. 273*, 25602−25611.
8. Feuer, G., and Straub, F. B. (1948) *Hung. Acta Physiol. 1*, 150−163.
9. Pardee, J., and Spudich, J. A. (1982) *J. Cell Biol. 93*, 648−654.
10. Pollard, T. D., and Weeds, A. G. (1984) *FEBS Lett. 170*, 94−98.
11. Carlier, M. F., Pantaloni, D., and Korn, E. D. (1987) *J. Biol. Chem. 262*, 3052−3059.
12. Carlier, M. F., Pantaloni, D., Evans, J. A., Lambooy, P. K., Korn, E. D., and Webb, M. R. (1988) *FEBS Lett. 235*, 211−214.
13. Pieper, U., and Wegner, A. (1996) *Biochemistry 35*, 4396−4402.
14. Melki, R., Fievez, S., and Carlier, M.-F. (1996) *Biochemistry 35*, 12038−12045.
15. Rickard, J. E., and Sheterline, P. (1986) *J. Mol. Biol. 180*, 273−279.
16. Carlier, M.-F., Pantaloni, D., and Korn, E. D. (1986) *J. Biol. Chem. 261*, 785−792.
17. Spudich, J. A., and Watt, S. (1971) *J. Biol. Chem. 246*, 4866−4871.
18. Pollard, T. D. (1984) *J. Cell Biol. 99*, 769−777.
19. MacLean-Fletcher, S., and Pollard, T. D. (1980) *Cell 20*, 329−341.
20. Kouyama, T., and Mihashi, K. (1981) *Eur. J. Biochem. 114*, 33−38.
21. Kaiser, D. A., Goldschmidt-Clermont, P. J., Levine, B. A., and Pollard, T. D. (1989) *Cell Motil. Cytoskeleton 14*, 251−262.
22. Almo, S. C., Pollard, T. D., Way, M., and Lattman, E. E. (1994) *J. Mol. Biol. 236*, 950−952.
23. Lin, D. C., and Lin, S. (1979) *Proc. Natl. Acad. Sci. U.S.A. 76*, 2345−2349.
24. Pollard, T. D., and Korn, E. D. (1973) *J. Biol. Chem. 248*, 4682−4690.
25. Martin, J. B., and Doty, D. M. (1949) *Anal. Chem. 21*, 965−967.
26. Barshop, A., Wrenn, R. F., and Frieden, C. (1983) *Anal. Biochem. 130*, 134−145.
27. Perelroizen, I., Didry, D., Christensen, H., Chua, N. H., and Carlier, M. F. (1996) *J. Biol. Chem. 271*, 12302−12309.
28. Pollard, T. D. (1986) *J. Cell Biol. 103*, 2747−2754.
29. Andrianantoandro, E., Blanchoin, L., Sept, D., McCammon, J. A., and Pollard, T. D. (2001) *J. Mol. Biol.*, in press.
30. Coue, M., and Korn, E. D. (1986) *J. Biol. Chem. 261*, 3628−3631.
31. Pollard, T. D., and Cooper, J. A. (1984) *Biochemistry 23*, 6631−6641.
32. Gutsche-Perelroizen, I., Lepault, J., Ott, A., and Carlier, M. F. (1999) *J. Biol. Chem. 274*, 6234−6243.
33. Kaiser, D. A., Vinson, V. K., Murphy, D. B., and Pollard, T. D. (1999) *J. Cell Sci. 112*, 3779−3790.
34. Kaiser, D. A., Sato, M., Ebert, R., and Pollard, T. D. (1986) *J. Cell Biol. 102*, 221−226.
35. Pantaloni, D., and Carlier, M. F. (1993) *Cell 75*, 1007−1014.
36. Kang, F., Purich, D. L., and Southwick, F. S. (1999) *J. Biol. Chem. 274*, 36963−36972.
37. Schutt, C., Myslik, J. C., Rozychi, M. D., Goonesekere, N. C. W., and Lindberg, U. (1993) *Nature 365*, 810−816.
38. Holmes, K. C., Popp, D., Gebhard, W., and Kabsch, W. (1990) *Nature 347*, 44−49.
39. Vinson, V. K., De La Cruz, E. M., Higgs, H. N., and Pollard, T. D. (1998) *Biochemistry 37*, 10871−10880.
40. Perelroizen, I., Marchand, J. B., Blanchoin, L., Didry, D., and Carlier, M. F. (1994) *Biochemistry 33*, 8472−8478.
41. Belmont, L. D., Orlova, A., Drubin, D. G., and Egelman, E. H. (1999) *Proc. Natl. Acad. Sci. U.S.A. 96*, 29−34.
42. Otterbein, L. R., Graceffa, P., and Dominquez, R. (2001) *Science 293*, 708−711.
43. Blanchoin, L., and Pollard, T. D. (1999) *J. Biol. Chem. 274*, 15538−15546.

BI011214B